TU Delft

Delft University of Technology

Influence of internal oscillations on force sensing in coil springs

van der Weijde, Joost; van Ostayen, Ron; Vallery, Heike

DOI
10.1109/LRA.2017.2665684

Publication date
2017

Document Version
Accepted author manuscript

Published in
IEEE Robotics and Automation Letters

Citation (APA)
van der Weijde, J., van Ostayen, R., & Vallery, H. (2017). Influence of internal oscillations on force sensing in coil springs. *IEEE Robotics and Automation Letters*, *2*(3), 1466-1471. https://doi.org/10.1109/LRA.2017.2665684

Important note
To cite this publication, please use the final published version (if applicable).
Please check the document version above.

Copyright
Other than for strictly personal use, it is not permitted to download, forward or distribute the text or part of it, without the consent of the author(s) and/or copyright holder(s), unless the work is under an open content license such as Creative Commons.

Takedown policy
Please contact us and provide details if you believe this document breaches copyrights.
We will remove access to the work immediately and investigate your claim.

This work is downloaded from Delft University of Technology.
For technical reasons the number of authors shown on this cover page is limited to a maximum of 10.

"(c) 2017 IEEE. Personal use of this material is permitted. Permission from IEEE must be obtained for all other users, including reprinting/ republishing this material for advertising or promotional purposes, creating new collective works for resale or redistribution to servers or lists, or reuse of any copyrighted components of this work in other works."

DOI: 10.1109/LRA.2017.2665684

Influence of Internal Oscillations on Force Sensing in Coil Springs

Joost van der Weijde, Ron van Ostayen and Heike Vallery

***Abstract*—Coil springs are a common element in compliant actuators. For closed-loop control, the force of the coil spring has to be measured. Typically, deflection sensors indirectly measure this force. Implicitly, this assumes that the coil spring is a pure stiffness, without any mass. In reality, internal oscillations can occur due to impacts or other excitations of the spring's resonance frequencies. This paper investigates the reliability of different force sensing methods for coil springs that are oscillating internally. In addition to standard sensing via strain gauges or deflection sensors, also a new type of sensing is included, namely force estimation via the spring's own electrical inductance. First, a lumped-mass model is used in simulations of three realistic conditions a coil spring might be subjected to in robotic applications. Second, a hardware experiment is conducted for one condition. Key effects predicted by the model are also found in the experiment, confirming the model's validity. Results show that for all sensors, the increase in measuring uncertainty due to internal oscillations is of the same order of magnitude as typical sensors' measuring uncertainty.**

***Index Terms*—Force and Tactile Sensing, Force Control, Compliance and Impedance Control**

I. INTRODUCTION

MORE and more robotic designs use physical compliance to enhance impedance-controlled interaction, for example around humans [1], [2]. Prominent examples are the Series Elastic Actuator (SEA) [3], [4] and Parallel Elastic Actuators. Mostly, these robots rely on closed-loop force control, requiring force sensing.

Commercially available force sensors often measure force by means of strain gauges. We call this "direct" force sensing, because only negligible deformations are required. Strain gauges exist of deformable resistors. They are typically used in combination with a structure, where the relation between strain on its surfaces and force at the end points is well known. This structure is typically an S-beam. Another commercial variant of force sensors employs the piezoelectric principle, which enables high precision and stiffness.

Dedicated force sensors are rare in the drive train of SEAs (for example found in [5]). Instead, force sensing in SEAs is mostly performed indirectly, by measuring deformation of the compliant elements. With coil springs as compliant elements, force sensing is simplified by exploiting Hooke's law and linearly relating force to spring deflection. This requires additional deflection sensor elements, e.g. encoders [2], [6] or potentiometers [7], [8], [9]. Ideally, coil spring deflection is measured directly, for example by placing linear potentiometers. A more indirect option to measure spring deflection in a robotic structure is to take the difference between measurements of two encoders placed on either side of the spring. A SEA typically has those two encoders in its drive train: one motor encoder and one joint encoder. This method relies on the (often incorrect) assumption that any further compliance or backlash in the drive train is negligible.

As a potentially cheaper and simpler sensor, we recently suggested a method to measure force using self-sensing of a metal coil spring, via its inductance [10]. This work, which included the theoretical background of the sensing principle, follows up on earlier empirical work by [11]. This sensing principle has not yet been applied apart from these papers, so its properties still need further investigation. Furthermore, this method is also based on deflection, but does not suffer from uncertainties introduced by the drive train.

What deflection-based sensing methods for spring force in robotics have in common is that they ignore spring mass and thereby inertial effects. Such effects can lead to internal oscillations of coil springs [12], [13], [14], in particular induced by collisions or harmonic excitation near the spring's resonance frequencies. An argument to neglect these internal vibrations is damping. In fact, [12] mentions several causes for damping in coil springs, like hysteresis in the spring material, air damping, friction in the end turns, and loss of energy in the supports. However, finding an actual value for damping requires experimental identification. Also, according to [12], damping in steel coil springs does not significantly change resonance frequencies, and amplification due to resonance may still be as high as 300.

So far, it has not been investigated in how far such oscillations influence force measurement in coil springs, neither for conventional deflection-based sensing, nor for inductance-based sensing. Such knowledge could be beneficial to judge relevance of these oscillations for particular applications, for example SEAs or parallel elastic actuators in robotic devices, or controlled car suspension systems. It can guide the choice of spring designs, sensing principles, sensor locations, or control schemes that are robust to the found uncertainties.

In this paper, we quantify how the different force sensing principles behave immediately following a collision or in response to excitation at a resonance frequency. For this analysis,

Manuscript received: September, 10, 2016; Revised December, 17, 2016; Accepted January, 18, 2017.

This paper was recommended for publication by Editor John Wen upon evaluation of the Associate Editor and Reviewers' comments.

Part of the research leading to these results has received funding from the European Union's Marie-Curie career integration grant PCIG13-GA-2013-618899

All authors are with the Faculty of Mechanical, Maritime, and Materials Engineering, Delft University of Technology, The Netherlands j.o.vanderweijde@tudelft.nl

Digital Object Identifier (DOI): see top of this page.

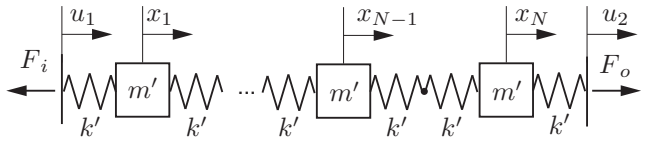

Fig. 1: N-dimensional mass-spring model of a coil spring, with inputs u_1 and u_2, positions x_1 to x_N. The individual masses m' are found by m/N and the individual stiffnesses k' are found by $2Nk$.

we first simulate responses using a lumped-mass model of the spring (Section II and Section III). Second, we verify model predictions via a hardware experiment (Section IV). Section V provides the results.

II. COIL SPRING MODEL

A. Mechanical Model

A coil spring has several Eigenfrequencies with corresponding mode shapes [13]. For our coil spring model, we only consider winding movements in axial direction, containing the first and most prominent mode shape.

The force transfer function for the axial direction of helical springs clamped on one side and with an imposed force at the other, with stiffness k and mass m, has for example been derived in [14]. They give the transmittance of force on one side of the spring F_i to the other side F_o as

$$\frac{F_o(j\omega)}{F_i(j\omega)} = \frac{2}{e^{j\omega\tau} + e^{-j\omega\tau}}, \tag{1}$$

where ω is the excitation frequency and τ is the dynamic spring characteristic:

$$\tau = \sqrt{m/k}. \tag{2}$$

Note that the dynamic spring characteristic τ is a physical property of a spring and should not be confused with the inverse of Eigenfrequencies, ω_n, of a coil spring. According to [12], Eigenfrequencies of clamped springs are found by

$$\omega_n = n\pi\sqrt{k/m}, \tag{3}$$

where n is a positive integer. Equation (1) describes the global input-output behavior, but the individual movement of each single winding remains unknown. Particularly for sensing via inductance, a nonuniform winding distribution could influence length measurement.

A lumped-mass model can represent the coil spring in more detail. We take each winding as an individual mass, with massless spring elements on either side. This results in an N-dimensional mass-spring system, where N is the number of windings (Fig. 1). Following [12], we consider damping negligible.

The absolute positions of the windings, x_1 to x_N, are collected in the vector $\mathbf{x}$ and the absolute positions of the end points of the spring are modeled as inputs u_1 and u_2 and collected in the vector $\mathbf{u}$. The vector $\mathbf{S}$ contains the deflections of all massless spring elements in between the masses and the matrix $\mathbf{K}$ contains their stiffness:

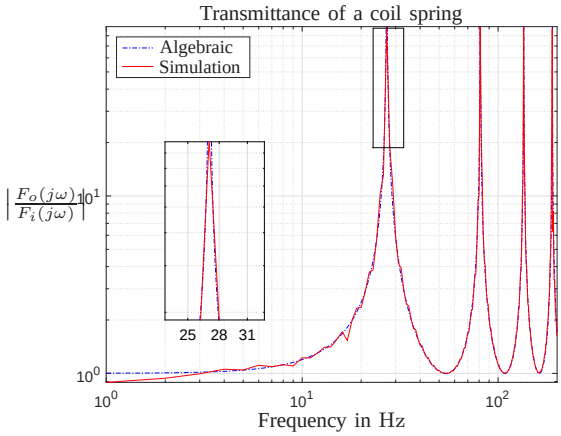

Fig. 2: Comparison of the algebraically calculated transmittance (blue dash-dotted line) with the transmittance of the model (red solid line). Both represent the transmittance of coil spring S_T in Table I.

$$\mathbf{S} = \begin{bmatrix} x_1 - u_1 \\ x_2 - x_1 \\ \vdots \\ x_N - x_{N-1} \\ u_2 - x_N \end{bmatrix}, \mathbf{K} = \text{diag}\begin{bmatrix} 2Nk \\ Nk \\ \vdots \\ Nk \\ 2Nk \end{bmatrix}, \tag{4}$$

The Jacobians of $\mathbf{S}$ with respect to $\mathbf{x}$ and $\mathbf{u}$, respectively $\mathbf{S}_{,\mathbf{x}}$ and $\mathbf{S}_{,\mathbf{u}}$, deliver the vector of resultant forces acting on each mass element:

$$\mathbf{F}_s = -\mathbf{S}_{,\mathbf{x}}{}^{\mathrm{T}}\mathbf{K}\left(\mathbf{S}_{,\mathbf{x}}\mathbf{x} + \mathbf{S}_{,\mathbf{u}}\mathbf{u}\right). \tag{5}$$

The equations of motion are

$$\frac{m}{N}\ddot{\mathbf{x}} = \mathbf{F}_s. \tag{6}$$

The spring forces at the end points, F_i and F_o, are

$$\begin{bmatrix} -F_i & F_o \end{bmatrix}^{\mathrm{T}} = \mathbf{S}_{,\mathbf{u}}{}^{\mathrm{T}}\mathbf{K}\left(\mathbf{S}_{,\mathbf{x}}\mathbf{x} + \mathbf{S}_{,\mathbf{u}}\mathbf{u}\right). \tag{7}$$

To validate the mechanical model, we compared its transmittance to the algebraic transmittance in (1). The transmittance of the model was obtained by applying a sinusoid force on one end of the coil spring, and investigating the response at the other end, for a frequency range from 1 to 200 Hz with steps of 1 Hz. We determined the amplitude and phase of the output by fitting the response on a sinusoid with the same frequency as the input. Fig. 2 illustrates the comparison in amplitude, using coil spring S_T in Table I.

B. Inductance Model

Investigation of inductance-based sensing requires a model of the inductance of a coil spring. We previously provided a comparison of several theoretical inductance-deflection relations [10]. We found that each theory captures the general behavior, given a uniform winding distribution. However, a vibrating coil spring has a nonuniform winding distribution. Maxwell's summation and integration of Neumann's equation are the only theories that capture the influence of a nonuniform winding distribution. Maxwell's summation fits best with the mechanical coil spring model, since it takes individual

TABLE I: Parameters of investigated coil springs.

	S_T	S_A
l_0	104 mm	81 mm
N	52	25
r	8 mm	8 mm
ρ	1 mm	1.6 mm
m	65 g	80 g
k	760 N/m	9100 N/m
l_{min}	196 mm	82 mm
l_{max}	264 mm	122 mm

windings into account. Therefore, we choose this model in the following.

Maxwell's method finds the inductance L of a coil by summation of all mutual inductances $M_{i,j}$ between individual windings i and j. One such mutual inductance is given by

$$M_{i,j} = -\mu_0 r \left(\left(\kappa_{i,j} - \frac{2}{\kappa_{i,j}} \right) K(\kappa_{i,j}) + \frac{2}{\kappa_{i,j}} E(\kappa_{i,j}) \right), \quad (8)$$

where μ_0 is the magnetic permeability of air, r the coil radius, $K(\kappa)$ and $E(\kappa)$ the elliptical integrals of the first and second kind, and

$$\kappa_{i,j}^2 = \frac{(2r)^2}{(2r)^2 + h_{i,j}^2}, \quad (9)$$

in which $h_{i,j}$ is the distance between the windings, resulting from the mechanical model. For the case of self inductance, where $i = j$, $h_{i,j}$ is given by the geometrical mean distance

$$h_{1,1} = {}^1\!/_2 \rho e^{-{}^1\!/_4}, \quad (10)$$

where ρ is the wire radius. The summation is now given by

$$L = \sum_{i=1}^{N} \sum_{j=1}^{N} M_{i,j}. \quad (11)$$

III. SIMULATION

A. Coil Spring Parameters

We investigate two different coil springs that originate from existing robotic platforms. More specifically, they form part of the drive trains of the respective platforms. Coil spring S_T is the antagonistic (front) spring of the SEA in the ankle of the humanoid robot TUlip [6]. Spring S_A is the parallel spring in the drive train of the lower-leg prosthetic ANGELAA [2]. Their relevant properties, rest length l_0, number of windings N, coil radius r, wire radius ρ, mass m, stiffness k and operating range [l_{min},l_{max}] in their respective systems are given in Table I.

B. Conditions

Typical use of coil springs in SEAs involves cases that result in internal oscillations. In the following, three such cases are modeled as conditions, and their respective influence on force sensing is investigated. We simulated each condition for 1 s and analyzed the final 0.25 s.

First, impacts on the structure of the robotic system, for example heel strike of walking robots, are noticed in the drive train. To simplify impact, we consider a coil spring initially moving at a uniform velocity when both ends simultaneously come to a sudden stop. We model this as the windings initially having a uniform distribution with a uniform velocity, with both position inputs fixed. We choose an initial velocity of 0.25 m/s, and we choose the extension for this condition to be at half of the application range.

Second, while extending or contracting the coil spring, the drive train might encounter a physical end stop. To model the behavior immediately after hitting such an end stop, we let the windings initially have uniform spacing, and the velocity be linearly distributed from zero to the extension or contraction velocity, while the inputs are both at a fixed position. A typical human or teen-/man-sized humanoid has a step time of about 1 second [15], [6]. We assume a case where the operating range is traversed within the step time. Therefore, we set the extension and contraction velocity to

$$\max(\dot{\mathbf{x}}_{\text{ext}}) = \max(-\dot{\mathbf{x}}_{\text{con}}) = {}^{l_{\text{max}} - l_{\text{min}}}\!/_1. \quad (12)$$

Both extension and contraction are evaluated. In these cases the end points are, respectively, fixed to the maximum and minimum extension.

Third, an actuator might apply a harmonic force or deflection on one of the inputs of the coil spring. If this sinusoid has a frequency in the neighborhood of one of the spring's Eigenfrequencies, the spring will start resonating. For this condition, we perform two harmonic excitations as a position input, at half of and on the first Eigenfrequency as calculated by (3), respectively with an amplitude of 1% and 0.1% of the position range of the coil spring. The other position input remains fixed.

C. Force Sensing Model

The sensor behavior is modeled by investigating the response of the coil spring at the points that are relevant for the respective sensors.

Force sensors would be applied at the ends of the coil springs, so their outputs are F_i and F_o as in (7).

For the inductance-based sensor, we assume the method given in [10]. A fit with parameters α and β, given by

$$\frac{1}{l_0 + \Delta l} = \alpha L + \beta, \quad (13)$$

captures the inductance-deflection behavior of a coil spring with a uniform winding distribution. While in a practical application, the parameters would be estimated with two or more inductance measurements at different deflections, here we use the theoretical inductance model in (11) with a uniform winding distribution to generate data to estimate α and β. A least-squares fit with a constraint to have the model match the static preload reduces the influence of fitting errors. The inductance response of a vibrating spring, i.e. the inductance with a nonuniform winding distribution, results from the same inductance model (11), with the simulated mechanical response as input. The resulting inductance is the input for (13), to estimate the deflection of the coil spring. Via the stiffness of the coil spring, we arrive at the inductance-based force measurement F_L.

Both encoders and linear potentiometers can measure net spring deflection Δl directly. As with the inductance-based method, force is found by multiplication of Δl with k, to arrive at F_x.

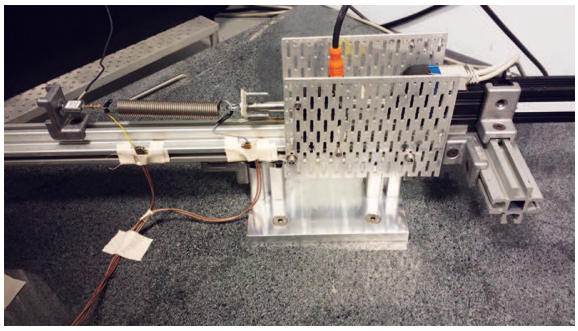

Fig. 3: The experimental setup: The spring is mounted between a linear actuator and a force sensor. It is also connected to an inductance meter, and a laser distance sensor measures deflection. The motor imposes harmonic oscillations at a range of frequencies, including the spring's first resonance.

D. Outcome Measures

Assessing the relative performance of a sensor requires a definition of nominal behavior and measurement range. Table I gives the operating range of the investigated coil springs. We define the nominal force F_{nom} as the maximum static force on the coil spring in their respective systems. It is found by

$$F_{\text{nom}} = k\,(l_{\text{max}} - l_0)\,. \tag{14}$$

We compare F_i, F_o and F_L to F_x for all simulated conditions. We choose the force that assumes a massless, and therefore static, spring, F_x, as a reference. The maximum force differences and the Root Mean Squared Difference (RMSD), indicate the uncertainty of the measurements. From these absolute values, relative measures are computed with respect to the nominal force F_{nom}.

IV. EXPERIMENT

A. Experimental Setup

To support the simulation in Section III, we conducted an experiment with a hardware setup that can reproduce one condition, namely excitation by a harmonic oscillation.

The S_T coil spring was suspended between a Dunkermotoren Servotube STA1116 Linear Actuator (LA), and a Futek LSB200 110 N Load Cell (LC). The relative deflection of the attachment point at the linear actuator was measured by a MicroEpsilon optoNCDT ILD 1401-10 Laser Distance Meter (LDM). A Matlab Simulink model controlled the LA at 500 Hz, and a National Instruments USB-6211 Data Acquisition box (DAQ) acquired the signals of the LC and the LDM at 2.5 kHz. An LCR43100 by Wayne Kerr measured the inductance using four-point measurement cables. The LCR43100 needs 445 ms per measurement. As illustrated in Fig. 3, all mechanical parts were mounted on a granite slab, to minimize any transfer of vibrations beyond the spring.

B. Protocol

First, the end effector of the LA was moved to the middle of the range of the LDM. This resulted in a preload of about 26 N. To reduce settling behavior during the experiment, we excited the coil spring at half of its Eigenfrequency for two minutes. Next, the stiffness and deflection offset of the coil spring were determined by force and position measurements at the end points of the LDM's range. The fitting parameters for (13) were determined using inductance measurements at those positions. We used a least-squares fit, with a constraint to have the fit match the static preload condition.

At the start, the LA held the preload position for 40 s. Next, it applied a series of sinusoid excitations around this position, each with a different frequency, for 40 s per frequency, with an amplitude of 1 mm. The frequencies were chosen such that the measurement time of the LCR43100 contained an integer number of periods of the excitation, starting with 1 and ending with 13 periods. For each condition, the DAQ and the LCR43100 were triggered simultaneously after the coil spring response had reached a steady state. Due to communication overhead, the LCR43100 took 59 samples per condition. At the end of the experiment, the LA held the preload position again for 40 s, to be able to identify any relaxation effects.

The 12th frequency was close to half the coil spring's first Eigenfrequency. We chose this moderate way of exciting the first Eigenfrequency, to avoid practical problems like impacting of windings.

C. Data Processing

In analogy to the simulation, the force at the load cell F_o can be compared to the force that results from deflection measurements F_x. For all excitations, the RMSD and the maximum deviation were calculated, relative to the nominal force as found by (14).

The inductance-based force measurements F_L require a different approach. In the dynamic cases, the LCR43100 measurement gives the averaged inductance over multiple periods of the excitation. The averaged inductance corresponds to an averaged force. Subtracting the deflection-based measurement of the preload provides the averaged force difference. For all three types of force measurement, the relative averaged force differences $\Delta\bar{F}_x$, $\Delta\bar{F}_o$ and $\Delta\bar{F}_L$were calculated, with their standard errors. Standard error $\sigma_{\bar{F}}$ is given by

$$\sigma_{\bar{F}} = {}^{\sigma}/_{\sqrt{n}}, \tag{15}$$

with standard deviation σ and the number of samples n.

V. RESULTS

Fig. 4 illustrates the responses of coil spring S_T to the 'heel strike' condition, the 'end stop' condition and the 'resonance' condition.

Table II and Table III respectively give the RMSDs and the maximum deviations of the force measurements for all conditions with respect to the massless spring assumption.

Fig. 5 shows the force data of the LC and force estimates using the LDM over time, for three excitation frequencies: 4.5, 20.2 and 27.0 Hz. Fig. 6 compares the RMSD and maximum difference between LC and LDM data (top) and the means and standard errors of all three measurement principles (bottom). The small frequency deviations in the second subplot facilitate clear reading of the error bars.

TABLE II: Root Mean Squared Differences of F_o, F_i and F_L with respect to F_x, relative to F_{nom}.

		F_i	F_o	F_L
S_T				
	heel strike	1.44%	1.44%	0.01%
	end stop collision max	0.22%	0.23%	0.01%
	end stop collision min	0.39%	0.39%	0.00%
	$1/2\,\omega_1$	0.37%	0.27%	0.00%
	ω_1	8.93%	8.94%	0.34%
S_A				
	heel strike	1.67%	1.67%	0.01%
	end stop collision max	0.15%	0.15%	0.01%
	end stop collision min	0.27%	0.27%	0.00%
	$1/2\,\omega_1$	0.78%	0.57%	0.02%
	ω_1	58.32%	58.36%	7.73%

TABLE III: Maximum deviations of F_o, F_i and F_L with respect to F_x, relative to F_{nom}.

		F_i	F_o	F_L
S_T				
	heel strike	3.11%	3.08%	0.00%
	end stop collision max	0.46%	0.44%	0.01%
	end stop collision min	0.85%	0.84%	0.00%
	$1/2\,\omega_1$	0.80%	0.42%	0.01%
	ω_1	14.39%	14.21%	0.00%
S_A				
	heel strike	3.77%	3.78%	-0.00%
	end stop collision max	0.46%	0.42%	0.01%
	end stop collision min	0.60%	0.61%	-0.00%
	$1/2\,\omega_1$	1.69%	0.94%	0.04%
	ω_1	93.05%	96.41%	0.03%

VI. DISCUSSION

Results indicate that internal oscillations in coil springs increase the measurement uncertainty of sensors for spring force. However, typical position and force sensors have an uncertainty of about 0.2%. Table II and Table III show that, in simulation, uncertainties due to internal oscillations not caused by harmonic excitation at a resonance frequency remain in the same order of magnitude. This holds true for all sensors, including the new sensing principle via inductance. In practice, the RMSD and maximum difference are larger, but still not exceeding 2 and 5%, respectively.

The differences between input and output forces confirm the well-known fact that in order to promote control stability when using a dedicated force sensor, such a sensor should preferably be placed at the motor side of the spring, avoiding non-collocated actuation and sensing [16].

The double set of data points in Fig. 6 at 0 Hz quantifies the relaxation during the experiment. We consider it negligible as it remains within the sensors' uncertainty.

For inductance-based force sensing, an interesting observation can be made: nonuniform winding distribution results in a negative inductance bias. Nonuniformity, so local winding density variation, changes each winding's contribution to the total inductance. While this change can be both positive and negative, the inverse proportional influence on inductance lets the inductance increase exceed the magnitude of the decrease. A higher inductance compared to uniform distribution, on which the fit is based, makes the coil appear shorter than it actually is, resulting in a lower average force estimate. Both in simulation and the hardware experiment, the effect is clearly visible at harmonic excitation at half the first resonance frequency, as illustrated in Fig. 6.

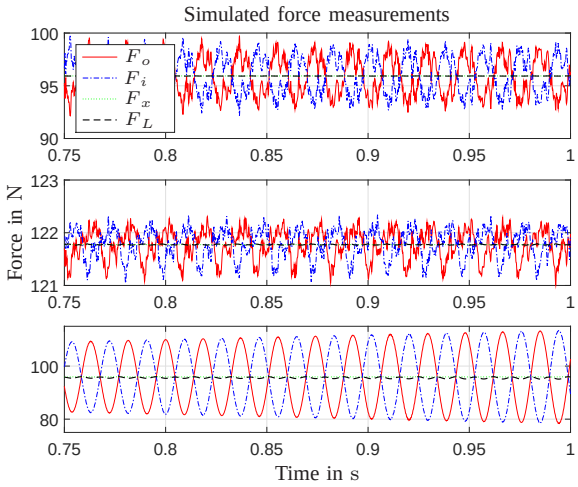

Fig. 4: Simulated force measurements for three excitation cases. The three subplots respectively contain the heel strike, the end-stop collision when extending and the excitation at the first Eigenfrequency. The red solid lines are the output forces F_o as in (7), the blue dash-dotted lines are the input forces F_i as in (7), the green dotted lines are the measured forces via direct position data F_x, and the black dashed lines are the measured forces via inductance data F_L.

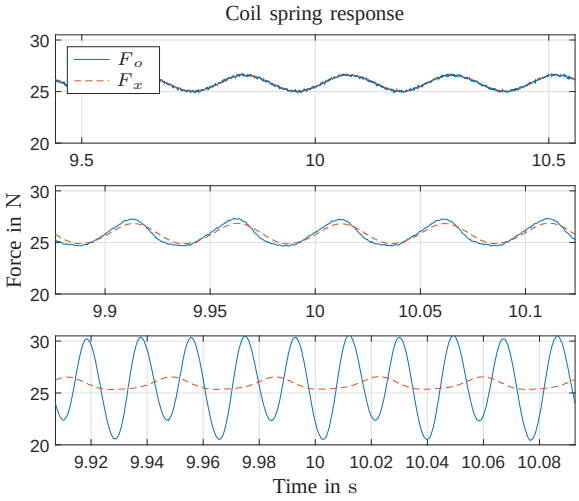

Fig. 5: Raw force measurements from a load cell and a laser distance meter, for three excitations: 4.5, 20.2 and 27.0 Hz.

While the force differences between F_o and F_x are visible in the RMSD and maximum difference in Fig. 6, the averaged values do not seem to differ. The inductance bias, however, is clearly visible at 27 Hz, when the first Eigenfrequency is being excited; averaging does not eliminate this bias. Future research could include measuring RMSD and maximum difference for inductance-based force sensing, using a faster inductance measuring device.

The simulation data and the data of the last subplot in Fig. 5 clearly show a large contribution of Eigenfrequencies calculated by (3) in the LC signal.

Although the observation of the bias may be of theoretical value, any resonance-induced bias in inductance sensing with respect to direct deflection sensing is negligible compared to the difference between the forces at the input and at the output side of the spring. Once resonance effects are so strong that

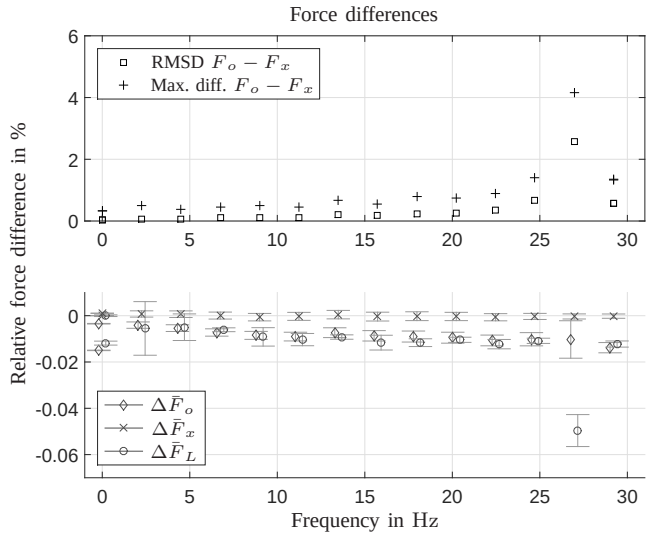

Fig. 6: Relative force measurement performance from a LC F_o, LDM F_x and an inductance meter F_L. The first subplot indicates the difference over time between the LC and the LDM, in the form of the RMSD and the maximum difference. The second subplot gives the relative averaged force measurements $\Delta\bar{F}_o$, $\Delta\bar{F}_x$ and $\Delta\bar{F}_L$.

the two ends of the spring do not exhibit comparable forces, conventional force control as in a SEA has little meaning. Based on this experiment, resonance-induced differences between inductance-based and conventional deflection sensing have no practical relevance.

Another, general indication from this study is that hardware and control designers should not only avoid excitation of a device's structural resonance frequencies, but also excitation of coil spring's own Eigenfrequencies in the system, at least if these springs are used for force sensing. Note that these Eigenfrequencies are not simply found by inverting (2), but from (3). Ways to mitigate oscillations in coil springs would be to purposefully introduce physical damping in the coil spring, for example by material choice or clamping conditions. Application of a low-pass filter below the first Eigenfrequency of the coil spring might help as well, but this reduces force control bandwidth. Notch filters or inverting the sensor model might be another option but would require specific knowledge on the used coil springs. In future work, we aim to identify and mitigate coil spring internal oscillation effects in a controlled system.

VII. CONCLUSION

In this paper, we showed how collisions and resonance effects can affect force sensing in coil springs. We used a lumped-mass model to simulate such internal oscillations in the spring's axial direction, in three different practically relevant conditions. An experiment confirmed expectations for one condition.

First, results indicate that internal oscillations can result in notably different forces at either end points of the coil spring, and therefore increase the uncertainty of sensor readings. Second, the increase in uncertainty for each measurement method has the same order of magnitude as the measuring uncertainty under normal conditions. Third, the recently introduced inductance-based force sensing gives very similar results as sensing based on direct measurement of spring deflection. This is true even in the presence of large internal oscillations and non-uniformity of the windings.

Incorporation of this knowledge into design and control strategies of robots may increase their safety and reliability.

ACKNOWLEDGMENT

We would like to thank Just Herder and Robert Babuska for their advice.

REFERENCES

[1] R. v. Ham, T. G. Sugar, B. Vanderborght, K. W. Hollander, and D. Lefeber, "Compliant actuator designs," *IEEE Robotics Automation Magazine*, vol. 16, no. 3, pp. 81–94, September 2009.

[2] S. Pfeifer, A. Pagel, R. Riener, and H. Vallery, "Actuator with Angle-Dependent Elasticity for Biomimetic Transfemoral Prostheses," *IEEE/ASME Transactions on Mechatronics*, vol. 20, no. 3, pp. 1384—1394, 2014.

[3] G. Pratt and M. Williamson, "Series elastic actuators," *Proceedings 1995 IEEE/RSJ International Conference on Intelligent Robots and Systems. Human Robot Interaction and Cooperative Robots*, vol. 1, pp. 399–406, 1995.

[4] H. Vallery, J. Veneman, E. van Asseldonk, R. Ekkelenkamp, M. Buss, and H. van Der Kooij, "Compliant actuation of rehabilitation robots," *IEEE Robotics Automation Magazine*, vol. 15, no. 3, pp. 60–69, September 2008.

[5] T. Mergner, G. Schweigart, and L. Fennell, "Vestibular humanoid postural control," *Journal of Physiology - Paris*, vol. 103, pp. 178–194, 2009.

[6] T. de Boer, "Foot placement in robotic bipedal locomotion," Ph.D. dissertation, Delft University of Technology, Netherlands, 2012.

[7] J. F. Veneman, R. Ekkelenkamp, R. Kruidhof, F. C. van der Helm, and H. van der Kooij, "A series elastic- and bowden-cable-based actuation system for use as torque actuator in exoskeleton-type robots," *The International Journal of Robotics Research*, vol. 25, no. 3, pp. 261–281, 2006.

[8] J. Pratt, P. Dilworth, and G. Pratt, "Virtual model control of a bipedal walking robot," in *Proceedings of International Conference on Robotics and Automation*, vol. 1. IEEE, 1997, pp. 193–198.

[9] D. W. Robinson, "Design and analysis of series elasticity in closed-loop actuator force control," Ph.D. dissertation, Massachusetts Institute of Technology, 2000.

[10] J. O. v. d. Weijde, E. Vlasblom, P. Dobbe, H. Vallery, and M. Fritschi, "Force Sensing for Compliant Actuators using Coil Spring Inductance," *IEEE International Conference on Intelligent Robots and Systems (IROS)*, pp. 2692–2697, September 2015.

[11] H. Kim, Y. Han, D.-y. Lee, J.-I. Ha, and K.-J. Cho, "Sensorless displacement estimation of a shape memory alloy coil spring actuator using inductance," *Smart Materials and Structures*, vol. 22, no. 2, p. 025001, 2013.

[12] A. M. Wahl, *Mechanical Springs*, 2nd ed. New York: McGraw-Hill, 1963.

[13] J. Lee and D. J. Thompson, "Dynamic Stiffness Formulation, Free Vibration and Wave Motion of Helical Springs," *Journal of Sound and Vibration*, vol. 239, no. 2, pp. 297–320, Jan. 2001.

[14] B. L. Johnson and E. E. Stewart, "Transfer functions for helical springs," *Journal of Engineering for Industry*, vol. 91, no. 4, pp. 1011—1016, 1969.

[15] O. Beauchet, C. Annweiler, Y. Lecordroch, G. Allali, V. Dubost, F. R. Herrmann, and R. W. Kressig, "Walking speed-related changes in stride time variability: effects of decreased speed," *Journal of NeuroEngineering and Rehabilitation*, vol. 6, no. 1, pp. 1–6, 2009.

[16] E. Colgate and N. Hogan, "An analysis of contact instability in terms of passive physical equivalents," in *Robotics and Automation, 1989. Proceedings., 1989 IEEE International Conference on*, May 1989, pp. 404–409 vol.1.